iJRASET
International Journal For Research in Applied Science and Engineering Technology



INTERNATIONAL JOURNAL FOR RESEARCH

IN APPLIED SCIENCE & ENGINEERING TECHNOLOGY

Volume: 13 **Issue:** VII **Month of publication:** July 2025

DOI: https://doi.org/10.22214/ijraset.2025.73227

www.ijraset.com

Call: 08813907089 | E-mail ID: ijraset@gmail.com

International Journal for Research in Applied Science & Engineering Technology (IJRASET)
ISSN: 2321-9653; IC Value: 45.98; SJ Impact Factor: 7.538
Volume 13 Issue VII July 2025- Available at www.ijraset.com

Role of Calcination Temperature on the Photocatalytic Activity of Zinc Tungstate Nanoparticles Synthesized by a Novel Route

Remya Muralimanohar[1], Sreelekshmi S[2], S Saravana Kumar[3]
[1, 3]*Department of Physics, N S S College, Pandalam, Research Centre - University of Kerala, 689501, India*
[2]*Department of Physics, Amrita Vishwa Vidyapeetham, Amrithapuri 690525, India*

Abstract: ***The studies on photocatalysts such as TiO2, ZnO, ZnWO4 have suggested that the crystallinity, surface area, phase purity, electron – hole recombination rate etc. play key roles in their catalytic activity. In the present work, the effect of calcination temperature on the photocatalytic activity of ZnWO4 nanoparticles synthesized by calcining ZnO and WO3 nanoparticle mixture is explored. The structural characterization of the samples were carried out using X-Ray Diffraction (XRD) and Raman techniques. Photocatalytic activity of the samples were studied on the photodegradation of Methylene Blue. The pseudo-first-order rate constant, kapp(min-1),was calculated from the slope of ln (Co/Ct) versus irradiation time t. From the study of photodegradation of MB in the presence of ZnWO4 nanoparticles, it was observed that the samples calcined at 8000C displayed more photocatalytic activity compared to other samples***
Keywords: $ZnWO_4$; Calcination; Methylene Blue; Photocatalysis; Phase-purity.

I. INTRODUCTION

Industrial revolution and population explosion highly expedited the scenario of environmental pollution globally. Among the other hazardous wastes dumped into the ecosystem, organic dye pollutants pose a major threat due to their entry into the water cycle as textile effluents. Since these toxic and carcinogenic pollutants have a complex chemical structure and very low biodegradability, simple filtration processes are of little use. The removal of such materials using green routes in a cost-effective manner is a trending topic of the recent times in waste water management regime [1].

Here, nanomaterials come into the picture for environmental remediation due to its ability to induce photocatalytic oxidation of organic pollutants over their surface under solar or ultraviolet light irradiation [2]. Nanomaterials possess high surface area, short intraparticle diffusion distances and interesting surface chemistry [3]; hence, they readily adsorb dye molecules [4]. Consequently the development of semiconductor nanostructures as photocatalysts for sunlight utilization is gaining popularity to address the global energy deficit. TiO_2, ZnO, $ZnWO_4$ etc. are most commonly used to achieve this purpose [5-8].

$ZnWO_4$ has many unique properties like high light yield, average refractive index, [9,10] short decay time, high photosensitivity, excellent chemical stability and non-toxicity which makes it a promising candidate to accomplish photocatalytic degradation of organic pollutants. Hence vast research efforts have been dedicated in the last few years for the synthesis of $ZnWO_4$ nanoparticles as efficient visible light photocatalysts.

$ZnWO_4$ can be synthesized from various precursors using different synthesis methods. Synthesis route plays an important role deciding the morphology, crystallinity and particle size distribution of the material. Formerly, $ZnWO_4$ has been prepared by various methods, such as: the mechano-chemical synthesis [11,12] the Czochralski technique [13], the hydrothermal synthesis [14], the solid state method [15], the spray-pyrolysis [16], the polymerized complex method [17], a molten salt route [18], co-precipitation [19], the sol-gel method [20], and electro-spinning [21]. Surface modification is brought about by means of changing annealing temperature [22].

In the present study nanoparticles of ZnO and WO_3 were synthesized by wet chemical synthesis method. Then equimolar mixtures of nanoparticles of ZnO and WO_3 were milled and calcined at different temperatures. This method provides a good control over the tailoring of size and phase as size of ZnO and WO_3 nanoparticles can be easily controlled by chemical precipitation technique. Also, this method is comparatively simple and inexpensive. Multiple intermediate milling steps helps in increasing the homogeneity of the sample [23]. Also, the effect of calcination temperature on the phase purity of the as-prepared samples and their influence on photocatalytic degradation efficiency were investigated.

©IJRASET: All Rights are Reserved

ISSN: 2321-9653; IC Value: 45.98; SJ Impact Factor: 7.538
Volume 13 Issue VII July 2025- Available at www.ijraset.com

II. MATERIALS AND METHODS

A. *Materials*

$ZnWO_4$ was prepared by means of conventional solid state reaction method where ZnO and WO_3 nanopowders were ground and calcined at a high temperature. ZnO nanoparticles were synthesized by chemical precipitation method from $ZnC_4H_6O_4$ and NaOH precursors using EDTA as capping agent and WO_3 nanoparticles from Na_2WO_4 and HNO_3 precursors. Aqueous medium was maintained throughout the reaction using deionized water.

$ZnC_4H_6O_4$, NaOH, EDTA, Na_2WO_4, HNO_3 and Methylene Blue dye were purchased from Merck. All reagents were of Analytical Grade and used without further purification.

B. *Methods*

20 ml of 0.5 M solution of $ZnC_4H_6O_4$ is added with 69 ml of deionized water and 1 ml EDTA solution was added dropwise by stirring. 1M NaOH solution was added to the solution. The precipitate was washed with deionized water and acetone by centrifuging at 5000 rpm, dried and ground to a fine powder. The sample was annealed at 850^0C in a Muffle Furnace to obtain ZnO nanoparticles.

10 ml of 0.1M Na_2WO_4 was stirred with 30 ml deionized water and 30 ml of con.HNO_3 was added dropwise. The precipitate was washed with deionized water and acetone by centrifuging at 5000rpm, dried and ground to a fine powder. The sample was annealed at 400^0C in a Muffle furnace to obtain WO_3 nanoparticles.

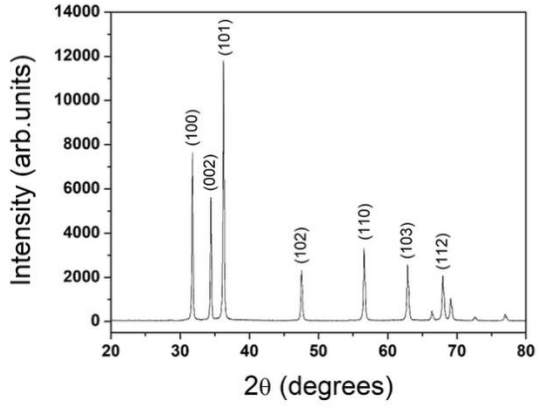
1:3 molar mixtures of ZnO and WO_3 nanopowders were crushed with Acetone using an agate mortar and pestle for almost one and a half hours. The sample is divided into four equal parts and calcined at 400^0C, 600^0C, 800^0C and 1000^0C for about 6 hours to get $ZnWO_4$ nanoparticles.

Structural characterization was done by XRD and HRTEM respectively. Raman spectrum was recorded to study the vibrational modes present in the structure of the sample. Photocatalytic study was carried out to check on the effectiveness of $ZnWO_4$ on the degradation of Methylene Blue dye. 80 W Mercury vapour lamp was used as the light source for conducting photocatalysis experiment. 1mM solution of Methylene Blue dye was prepared and a 30 ml aliquot was sonicated with 20 mg of $ZnWO_4$ nanoparticles. The mixture was kept under illumination for five hours and its degradation kinetics were studied using UV-Vis Absorption Spectrophotometer.

III. RESULTS AND DISCUSSION

A. *X-ray Diffraction Studies*

The X-ray diffraction pattern of nanoparticles of ZnO and WO_3 are shown in the Figure 1 (a) and 1 (b) respectively. The 2θ values obtained were compared with standard PDF values of cubic (No. 77-0191) and hexagonal (No. 89-1397) phases for ZnO and with standard PDF values of hexagonal (No. 75-2187), monoclinic (No. 83-0950) and orthorhombic phases of WO_3 (No. 43-0679). It was observed that ZnO nanoparticles of present study are in hexagonal or wurtzite phase and WO_3 nanoparticles in orthorhombic phase.



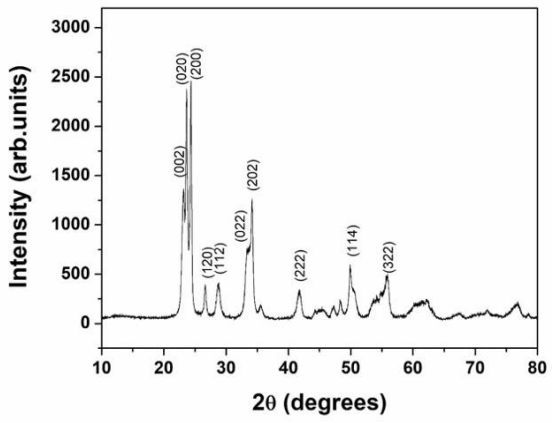


FIgure 1 (a). XRD pattern of nanoparticles of ZnO

Figure 1 (b). XRD pattern of nanoparticles of WO_3

©IJRASET: All Rights are Reserved | SJ Impact Factor 7.538 | ISRA Journal Impact Factor 7.894 |

ISSN: 2321-9653; IC Value: 45.98; SJ Impact Factor: 7.538
Volume 13 Issue VII July 2025- Available at www.ijraset.com

The XRD pattern of nanoparticles of $ZnWO_4$ calcined at 400^0 C, 600^0 C, 800^0 C and 1000^0 C are shown in the Figure 2. The 2θ values obtained were compared with standard PDF values of monoclinic and orthorhombic phases of $ZnWO_4$. It was observed that the samples calcined at 800^0 C and 1000^0C exhibited pure monoclinic phase (No. 73-0554) of zinc tungstate. The characteristic peaks of orthorhombic phase at 13.03^0 and 32.8^0 were absent in the XRD pattern of all the samples. The sample calcined at 400^0 C and 600^0C exhibited peaks at 23.19^0, 26.61^0 and 34.5^0 corresponding to reflections from (002), (120) and (202) planes of orthorhombic phase of WO_3.

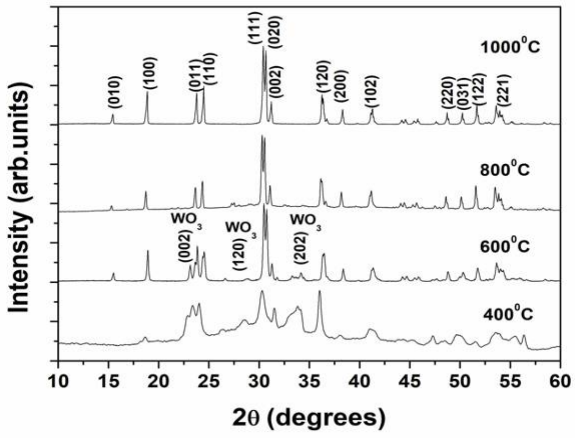


FIgure 2. XRD pattern of nanoparticles of $ZnWO_4$

It can be observed that WO_3 phase was retained in the samples calcined at 400^0 C and 600^0C and a complete transformation to $ZnWO_4$ was evident at 800^0C. The crystallite size of the samples was calculated using Debye-Scherrer equation [24] and is shown in the Table 1.

From the table, it can be understood that the crystallite size increases with increase in calcination temperature indicating the enhanced crystallinity. Faka et. al. [22] reported the preparation of $ZnWO_4$ nanoparticles using solution based synthetic route and obtained single phase $ZnWO_4$ nanoparticles at 600^0C. Huang et.al. [19] reported that calcination at 500^0C yielded phase pure $ZnWO_4$ powders synthesized by co-precipitation technique. It can be inferred that optimum calcination temperature to yield single phase $ZnWO_4$ nanoparticles depends on the synthesis methods.

B. HRTEM Studies

The TEM image, HRTEM image and SAED pattern of $ZnWO_4$ nanoparticles calcined at 800^0C are shown in the figures 3 (a), 3 (b) and 3 (c) respectively. The TEM image of individual nanoparticles show a particle size of approximately 50 nm and the HRTEM image show an interplanar spacing of 0.27 nm corresponding to (111) plane of $ZnWO_4$. The SAED pattern exhibits single spots indicating the phase purity of the samples.

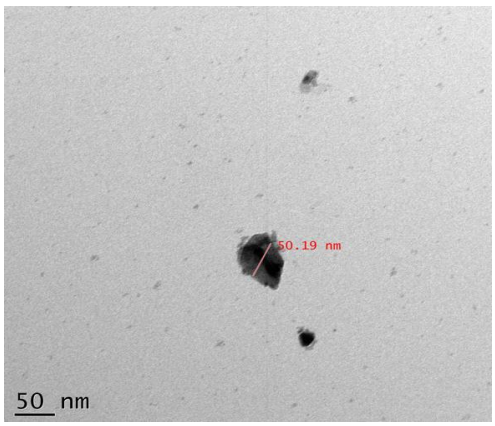


Figure 3 (a). TEM image of $ZnWO_4$ nanoparticles

©IJRASET: All Rights are Reserved | SJ Impact Factor 7.538 | ISRA Journal Impact Factor 7.894 |

ISSN: 2321-9653; IC Value: 45.98; SJ Impact Factor: 7.538
Volume 13 Issue VII July 2025- Available at www.ijraset.com

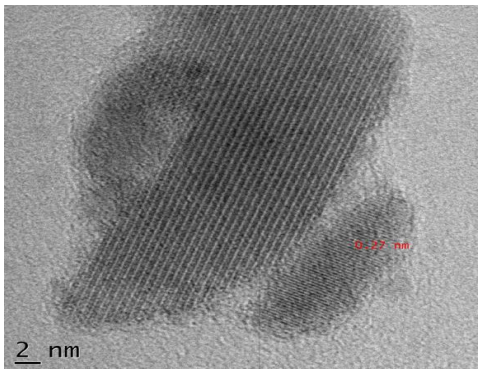


Figure 3 (b). HRTEM image of $ZnWO_4$ nanoparticles

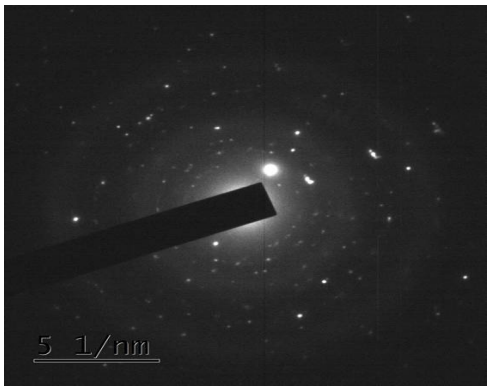
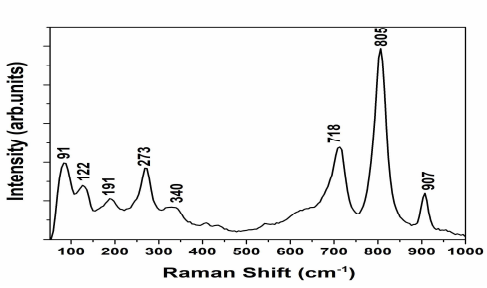


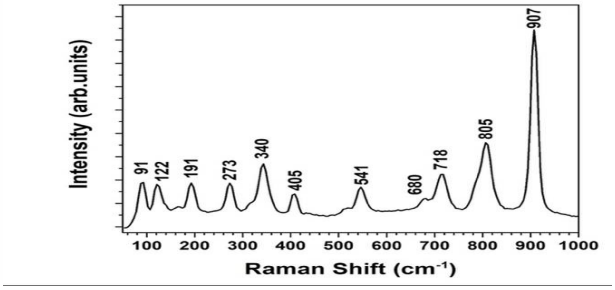
Figure 3 (c). SAED pattern of $ZnWO_4$ nanoparticles

C. Raman Studies

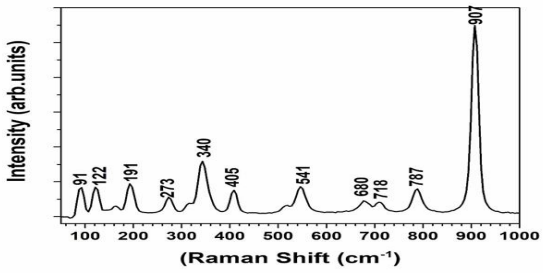
The Raman spectra of $ZnWO_4$ nanoparticles calcined at 400^0 C, 600^0 C, 800^0 C and 1000^0 C are shown in the figures 4 (a), 4 (b), 4 (c) and 4 (d) respectively.



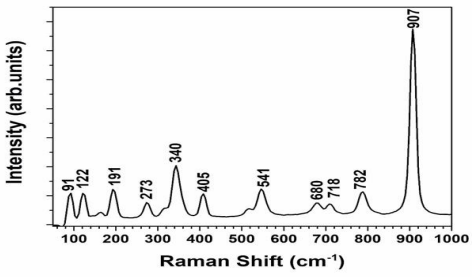
a) 400^0 C



b) 600^0 C



c) 800^0 C



d) 1000^0 C

Figure 4. Raman Spectra of $ZnWO_4$ nanoparticles calcined at 400^0C, 600^0 C. 800^0 C and 1000^0 C respectively

©IJRASET: All Rights are Reserved | SJ Impact Factor 7.538 | ISRA Journal Impact Factor 7.894 |

The Raman spectra of samples calcined at 400^0 C and 600^0C exhibited peaks around 91, 122, 191, 273, 340, 405, 541, 680, 718, 805 and 907 cm^{-1}. The peak at 805 cm^{-1} present in the Raman spectrum of the samples calcined at 400^0C and 600^0C are absent in that of the samples calcined at 800^0C and 1000^0C. Also, a peak at 787 cm^{-1} is present in the samples calcined at 800^0C and 1000^0C. The $ZnW0_4$ of present study is of wolframite structure, C_{2h} point symmetry, and P 2/ C space group symmetry with two formula groups per primitive cell. The group theory calculations predict 36 vibrations of species $8A_g + 10B_g + 8A_u + 10B_u$ in which all of the even (g) vibrations are Raman active and all of the odd vibrations (u) are IR active [25,26]. These vibrational modes are classified in two types: internal and external modes. The external vibrational modes are associated with the distorted octahedral [ZnO_6] clusters in the lattice while the internal vibrational modes are assigned to distorted octahedral [WO_6] clusters. The phonon frequencies of the external modes associated with Zn–O have lower frequencies compared to that associated with internal modes. This is due to the strong covalent nature of W–O bonds. The peak at 907 cm^{-1} can be ascribed to the symmetric stretching of O-W-O bond [27]. The peak at 718 cm^{-1} is assigned to A_g symmetric stretching of O-W-O bond. The peak around 787 cm^{-1} (in the spectra of samples calcined at 800^0 and 900^0C) can be ascribed to B_g asymmetric stretching of O-W-O bond [24]. The peak at 805 cm^{-1} observed in the Raman spectrum of the samples calcined at 400^0 and 600^0C can be attributed stretching vibrations of O-W-O of WO_3 indicating the presence of WO_3 in the sample [28]. The presence of WO_3 in the samples calcined at 600^0C is also observed in the XRD pattern.
The peaks at 405 cm^{-1} and 541 cm^{-1} corresponds to A_g and that at 405 cm^{-1} and 680 cm^{-1} corresponds to B_g stretching of long W-O bonds [29]. The Raman peaks at 122 cm^{-1} and 191 cm^{-1} can be ascribed to A_g and B_g modes corresponding to symmetric stretching of O-Zn-O bond. The peaks at 273 cm^{-1} and 340 cm^{-1} are assigned to be due to cationic sublattice vibrations [26]. These results suggest that the $ZnWO_4$ nanocrystals are structurally ordered in the short range and correspond to a wolframite-type monoclinic structure, which corroborate the results obtained from XRD analysis.

D. Photocatalytic activity of $ZnWO_4$ Nanoparticles

The absorption spectrum of methylene blue (without $ZnWO_4$ nanoparticles) before and after UV irradiation for 5 hours is shown in the Figure 5.

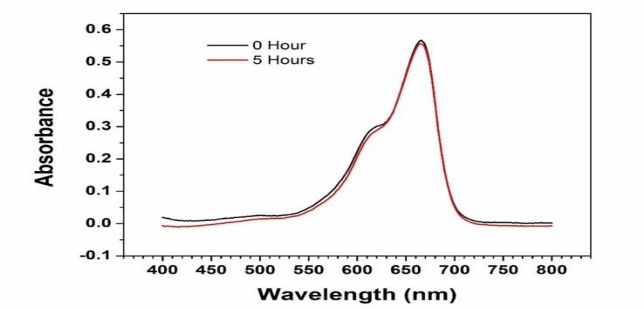


Figure 5. Absorption spectrum of Methylene Blue without $ZnWO_4$ nanoparticles

The spectrum shows intense absorption peak at 665 nm. The absorbance spectra of MeB dye after catalytic degradation by $ZnWO_4$ calcined at 400^0 C, 600^0 C, 800^0 C and 1000^0 C under irradiation with UV light for different time intervals are shown in the figures 6 (a), 6 (b), 6 (c) and 6 (d) respectively.

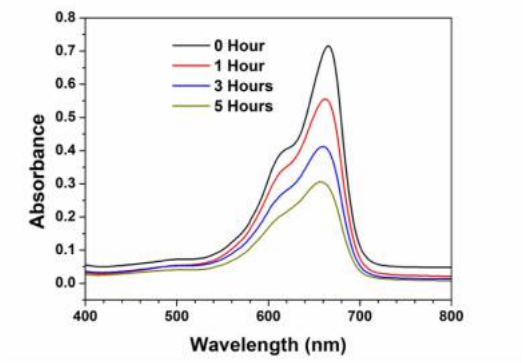


Figure 6 (a). Absorption spectra of Methylene blue with $ZnWO_4$ nanoparticles calcined at 400^0C

ISSN: 2321-9653; IC Value: 45.98; SJ Impact Factor: 7.538
Volume 13 Issue VII July 2025- Available at www.ijraset.com

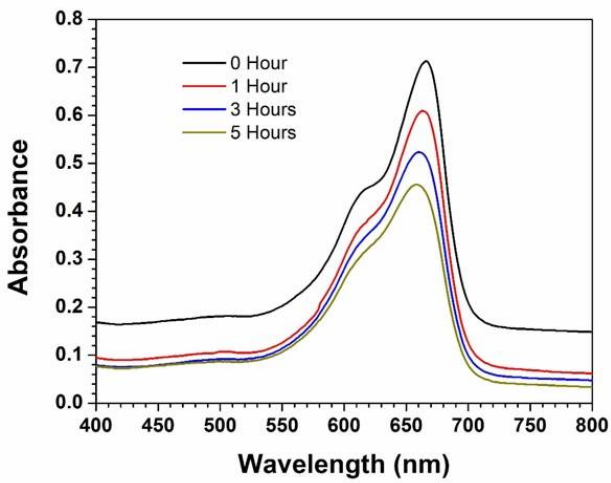


Figure 6 (b). Absorption spectra of Methylene blue with $ZnWO_4$ nanoparticles calcined at 600^0C

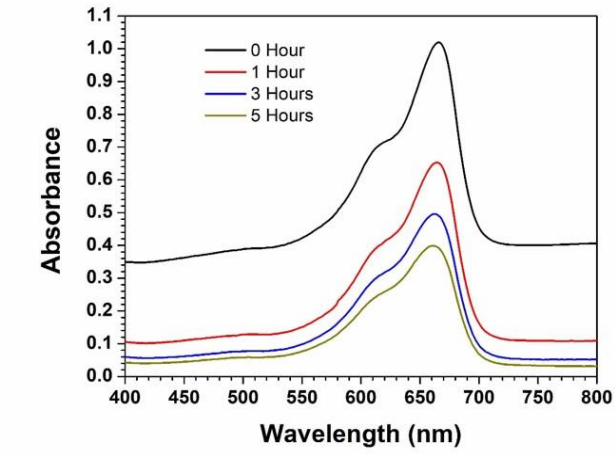


Figure 6 (c). Absorption spectra of Methylene blue with $ZnWO_4$ nanoparticles calcined at 800^0C

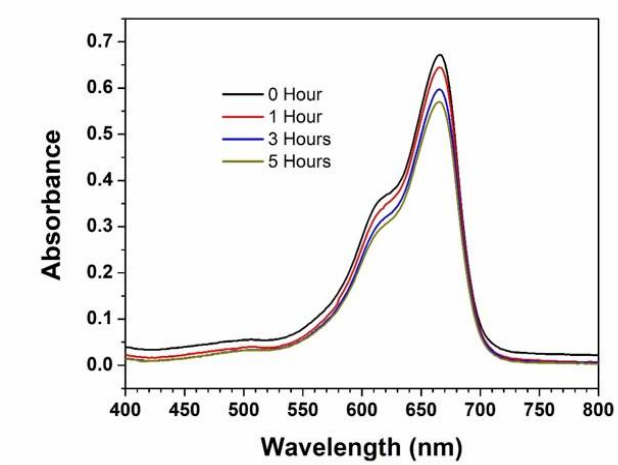


Figure 6 (d). Absorption spectra of Methylene blue with $ZnWO_4$ nanoparticles calcined at 1000^0C

From the figures, it can be observed that the intensity of the absorption peak decreases with time.

©IJRASET: All Rights are Reserved | SJ Impact Factor 7.538 | ISRA Journal Impact Factor 7.894 |

ISSN: 2321-9653; IC Value: 45.98; SJ Impact Factor: 7.538
Volume 13 Issue VII July 2025- Available at www.ijraset.com

The photocatalytic efficiency of $ZnWO_4$ nanoparticles were calculated using the equation,

MB colour removal (%) = $(C_o - C_t)/C_o \times 100$ [30,31],

where C_o is the initial concentration and C_t is the concentration at any irradiation time t (min). The plot showing the variation of photocatalytic efficiency of $ZnWO_4$ nanoparticles calcined at 400^0 C, 600^0 C, 800^0 C and 1000^0 C are shown the Figure 7.

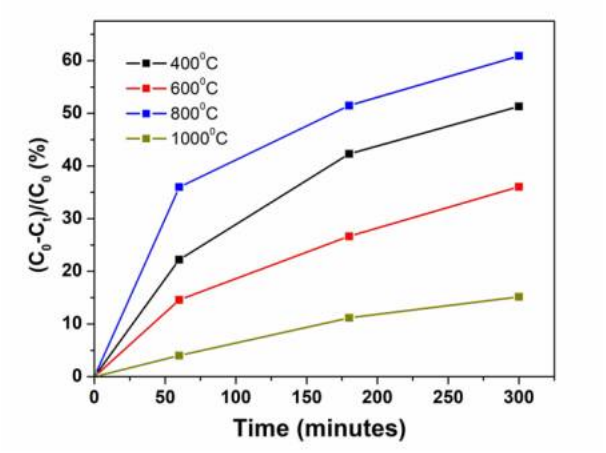


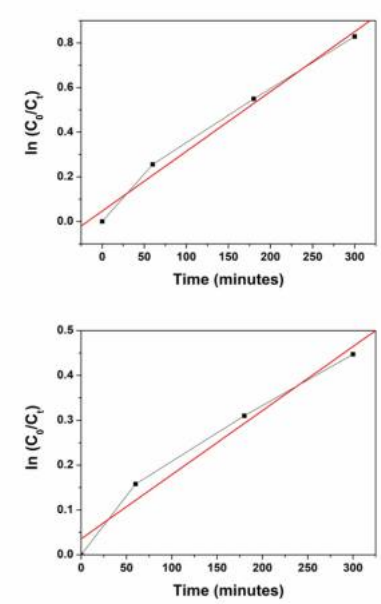
Figure 7. Photocatalytic efficiency of $ZnWO_4$ nanoparticles calcined at 400^0 C, 600^0 C, 800^0 C and 1000^0 C

From the figure, it can be observed that the samples calcined at 800^0C have maximum photocatalytic efficiency and those calcined at 1000^0C have minimum value.

The kinetics of the photocatalytic decolourization rate of MB was determined using the Langmuir–Hinshelwood kinetics model [32], as given in the equation given below,

$$\mathbf{ln(C_o/C_t) = k_{app}t}$$

The pseudo-first-order rate constant, $k_{app}(min^{-1})$ was calculated from the slope of ln (C_o/C_t) versus irradiation time t. The plot of $ln(C_o/C_t)$ versus time for the photocatalytic decolourization of MB by $ZnWO_4$ nanoparticles calcined at 400^0 C, 600^0 C, 800^0 C and 1000^0C are shown in the Figure 8.



©IJRASET: All Rights are Reserved | SJ Impact Factor 7.538 | ISRA Journal Impact Factor 7.894 |

ISSN: 2321-9653; IC Value: 45.98; SJ Impact Factor: 7.538
Volume 13 Issue VII July 2025- Available at www.ijraset.com

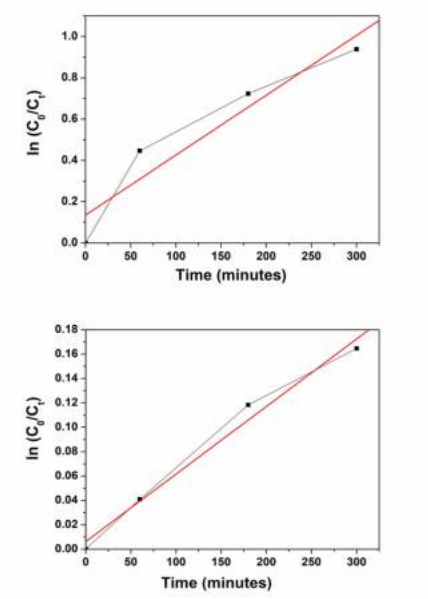


Figure 8. Plot of ln C_0/C_t vs time for $ZnWO_4$ samples calcined at 400^0C, 600^0C, 800^0C and 1000^0C respectively

The $k_{app}(min^{-1})$, rate constant values of $ZnWO_4$ nanoparticles calcined at 400^0C, 600^0C, 800^0C and 1000^0C were calculated to be 2.6 x 10^{-3}, 1.4 x 10^{-3}, 2.9 x 10^{-3} and 0.5 x 10^{-3} respectively.

From the study of photodegradation of MB in the presence of $ZnWO_4$ nanoparticles, it can be observed that the samples calcined at 800^0C show more photocatalytic activity and the samples calcined at 1000^0C exhibited poor catalysis. The samples calcined at 400^0C and 600^0C showed moderate photocatalytic activities. The light absorption and the migration of photo induced charge carriers are the major factors that determine the photocatalytic efficiency of a semiconductor [33]. The crystallinity, phase purity and crystallite or particle size plays a major role in the migration of charge carriers [19]. The XRD pattern and the Raman spectra of the samples calcined at 400^0C and 600^0C indicated the presence of WO_3 phases. The presence of WO_3 in the samples may modify the electronic structure and the crystallinity of the zinc tungstate nanoparticles and may result in the decrease in photocatalytic activity. The XRD pattern and the Raman spectrum of the samples calcined at 1000^0C revealed that the crystallite size and the crystallinity was increased. The increase in crystallite size and crystallinity decreases surface area, which in turn affects the catalytic activity.

IV. CONCLUSION

Photocatalytic reaction is a green technique for waste water treatment, performed in the presence of light and suitable catalyst which degrade the pollutant in water. In the present work, nanostructured $ZnWO_4$ were synthesized by calcining ZnO and WO_3 nanoparticles at 400^0 C, 600^0 C, 800^0 C and 1000^0 C. From the XRD pattern of $ZnWO_4$, it was observed that the samples calcined at 800^0 C and 1000^0C exhibited pure monoclinic phase of zinc tungstate while that at 400^0 C and 600^0 C exhibited reflection peaks corresponding to WO_3 also. The grain sizes of nanoparticles of $ZnWO_4$ were calculated using Debye-Scherrer equation. It was observed that the grain size of zinc tungstate nanoparticles increases with increase in calcining temperature. Results of Raman spectra analysis suggested that the $ZnWO_4$ nanocrystals calcined at 800^0 C and 1000^0C were structurally ordered in the short range and correspond to a wolframite-type monoclinic structure. The samples calcined at 400^0 C and 600^0 C exhibited Raman peaks corresponding to WO_3 phase. Photocatalytic activities of the samples were studied on the photodegradation of Methylene Blue. The photocatalytic efficiency and pseudo-first-order rate constant, $k_{app}(min^{-1})$ were calculated. It was observed that the samples calcined at 800^0 C show more photocatalytic activity and the samples calcined at 1000^0 C exhibited poor catalysis. The $ZnWO_4$ samples calcined at 800^0 C has phase purity compared to that calcined at 600^0 C and less grain size compared to that calcined at 1000^0 C. This may be the reason for the substantially high photocatalytic activity of $ZnWO_4$ samples calcined at 800^0 C compared to others.

V. ACKNOWLEDGEMENTS

First author acknowledges DST for providing financial assistance through Women Scientist Scheme-A (SR/WOS-A/PM-96/2018). Third author acknowledges DST-FIST for providing facility in the institution. Authors acknowledge the characterization facilities at

©IJRASET: All Rights are Reserved

SAIF- Cochin University of Science and Technology for the HRTEM studies, SAIF- Mahatma Gandhi University for the Raman Studies and CLIF- Kerala University for the XRD Studies.

REFERENCES

[1] Saratale R G, Rajesh Banu J, Shin H S, Bharagava R N and Saratale G D 2020 Textile Industry Wastewaters as Major Sources of Environmental Contamination: Bioremediation Approaches for Its Degradation and Detoxification. In: Saxena G, Bharagava R, Bioremediation of Industrial Waste for Environmental Safety, Springer Singapore 1 p.135
[2] Sadaf Bashir Khan and Shern Long Lee 2021 Nano Ex. 2 022002
[3] Xiaolei Qu, Pedro J.J. Alvarez, Qilin Li 2013 Water Res. 47 12 p.3931
[4] Homaeigohar S 2020 Nanomaterials 10 2 p.295
[5] Ohtani B, Ogawa Y and Nishimoto S 1997 J. Phys. Chem. B 101 19 p.3746
[6] Sonik Bhatia and Neha Verma 2017 Mater. Res. Bull. 95 p.468
[7] Huang G, Zhang C and Zhu Y 2007 J. Alloys Compd. 432 p.269
[8] Chunyang Li, Xiaodi Du, Yurong Shi and Zhenling Wang 2019 Micro Nano Lett. 14 5 p.496
[9] Hongbo Fu, Jie Lin, Liwu Zhang and Yongfa Zhu 2006 Appl. Catal. A: Gen. 306 p.58
[10] Pereira P F S, Gouveia A F, Assis M, De Oliveira R C, Pinatti I M, Penha M et al 2018 Phys. Chem. Chem. Phys. 20 p.1923
[11] Mancheva M, Iordanova R, and Dimitriev Y 2011 J. Alloys Compd. 509 p.15
[12] Dodd A, Mckinley A, Tsuzuki T and Saunders M 2009 J. Eur. Ceram. 29 1 p.139
[13] Oi T, Takagi K and Fukazawa T 1980 Appl. Phys. Lett. 36 p.278
[14] Buhl J C and Willgallis A 1986 Chem. Geol. 56 p.271
[15] Phani A R, Passacantando M, Lozzi L and Santucci S 2000 J. Mater. Sci. 35 19 p.4879
[16] Lou Z, Hao J and Cocivera M 2002 J. Lumin. 99 4 p.349
[17] Ryu Jeong Ho, Lim Chang and Auh Keun 2003 Mater. Lett. 57 9 p.1550
[18] Ran Songlin and Gao Lian 2006 Chem. Lett. 35 11 p.1312
[19] Huang G and Zhu Y 2007 Mater. Sci. Eng. B 139 p.201
[20] Wu Yan, Zhang Shi-cheng, Zhang Li-wu, Zhu Yong-fa 2007 Chem. Res. Chinese U. 23 4 p.465
[21] Keereeta Y, Thongtem T and Thongtem S 2011 J. Alloys Compd. 509 23 p.6689
[22] Faka V, Tsoumachidou S, Moschogiannaki M, Kiriakidis G, Poulios I and Binas V 2021 J. Photochem. Photobiol. A 406 p.113002
[23] Buekenhoudt A Kovalevsky, Luyten J and Snijkers F 2010 1.11 Basic Aspects in Inorganic Membrane Preparation Enrico Drioli and Lidietta Giorno Comprehensive Membrane Science and Engineering Elsevier 217
[24] Cullity B D and Stock S R 2001 Elements of X-ray Diffraction Third Edition. New York : Prentice-Hall
[25] Liu Y, Wang H, Chen G, Zhou Y D, Gu B Y and Hu B Q 1988 J. Appl. Phys. 64 p.4651
[26] Liu Meng-ting, Xiao En-cai, Lv Ji-qing, Qi Ze-ming, Yue Zhenxing, Chen Ying Chen et al 2020 J. Mater. Sci.: Mater. Electron 31 8 p.6192
[27] Kalinko A, Kuzmin A 2009 J. Lumin. 129 10 p.1144
[28] Errandonea D, Manjón F J, Garro N, Rodríguez-Hernández P, Radescu S, Mujica A, Muñoz A and Tu C Y 2008 Phys. Rev. B 78 054116
[29] Yajun Wang, Zhenxing Wang, Safdar Muhammad and Jun He 2012 CrystEngComm. 14 p.5065
[30] Pandurangan A, Kamala P, Uma S, Palanichamy M and Murugesan V 2001 Ind. J. Chem. Technol. 8 p.496
[31] Hinda Lachheb, Eric Puzenat, Ammar Houas, Mohamed Ksibi, Elimame Elaloui, Chantal Guillard et al 2002 Appl. Catal. B 39 1 p.75
[32] Molinari R, Argurio P, Bellardita M and Palmisano L 2017 3.5 Photocatalytic Processes in Membrane Reactors Enrico Drioli, Lidietta Giorno, Enrica Fontananova Comprehensive Membrane Science and Engineering Sec. Ed. Elsevier p.101
[33] Tang J, Zou Z and Ye J 2004 Angew. Chem. Int. Ed. 43 p.4463

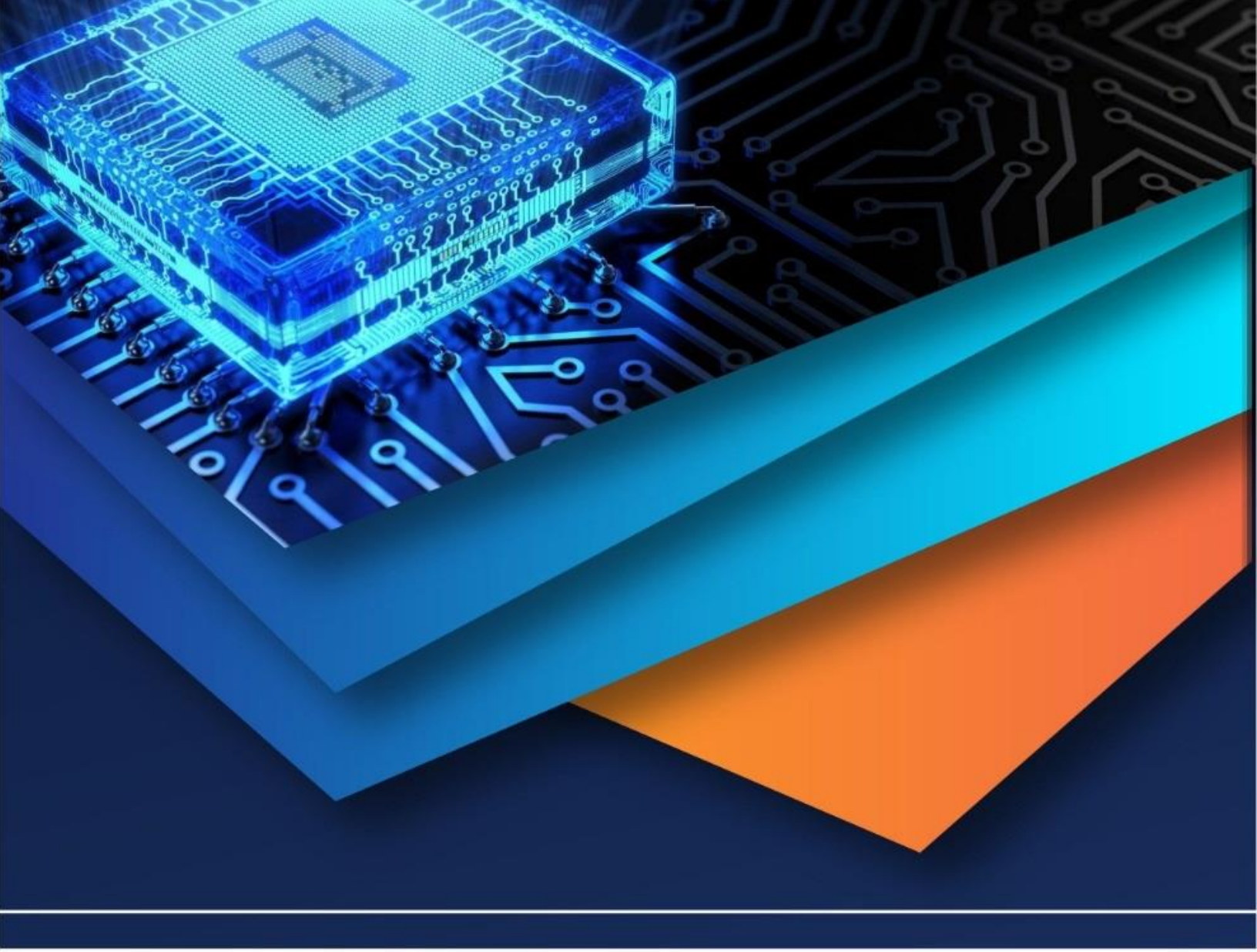
TABLES

Table 1

Calcination Temperature	Average Crystallite size (nm) (Debye-Scherrer)
400^0C	36
600^0C	48
800^0C	68
1000^0C	83

Table 1. Calcination temperature and average crystallite size of $ZnWO_4$ nanoparticles

©IJRASET: All Rights are Reserved | SJ Impact Factor 7.538 | ISRA Journal Impact Factor 7.894 |



10.22214/IJRASET

45.98

IMPACT FACTOR: 7.129

IMPACT FACTOR: 7.429

INTERNATIONAL JOURNAL FOR RESEARCH

IN APPLIED SCIENCE & ENGINEERING TECHNOLOGY

Call : 08813907089 (24*7 Support on Whatsapp)